X-ray emission from the outer planets: Albedo for scattering and fluorescence of solar X rays

T. E. Cravens,[1] J. Clark,[1] A. Bhardwaj,[2,3] R. Elsner,[2] J. H. Waite Jr.,[4] A. N. Maurellis,[5] G. R. Gladstone,[6] and G. Branduardi-Raymont[7]

Received 7 September 2005; revised 23 January 2006; accepted 3 February 2006; published 15 July 2006.

[1] Soft X-ray emission has been observed from the low-latitude "disk" of both Jupiter and Saturn as well as from the auroral regions of these planets. The disk emission as observed by ROSAT, the Chandra X-Ray Observatory, and XMM-Newton appears to be uniformly distributed across the disk and to be correlated with solar activity. These characteristics suggest that the disk X rays are produced by (1) the elastic scattering of solar X rays by atmospheric neutrals and (2) the absorption of solar X rays in the carbon K-shell followed by fluorescent emission. The carbon atoms are found in methane molecules located below the homopause. In this paper we present the results of calculations of the scattering albedo for soft X rays. We also show the calculated X-ray intensity for a range of atmospheric abundances for Jupiter and Saturn and for a number of solar irradiance spectra. The model calculations are compared with recent X-ray observations of Jupiter and Saturn. We conclude that the emission of soft X rays from the disks of Jupiter and Saturn can be largely explained by the scattering and fluorescence of solar soft X rays. We suggest that measured X-ray intensities from the disk regions of Jupiter and Saturn can be used to constrain both the absolute intensity and the spectrum of solar X rays.

Citation: Cravens, T. E., J. Clark, A. Bhardwaj, R. Elsner, J. H. Waite Jr., A. N. Maurellis, G. R. Gladstone, and G. Branduardi-Raymont (2006), X-ray emission from the outer planets: Albedo for scattering and fluorescence of solar X rays, *J. Geophys. Res.*, *111*, A07308, doi:10.1029/2005JA011413.

1. Introduction

[2] X-ray emission has been observed from Jupiter with the Einstein satellite [*Metzger et al.*, 1983], the ROSAT satellite [*Waite et al.*, 1994, 1997; *Gladstone et al.*, 1998; *Ness and Schmitt*, 2000], the XMM-Newton Observatory [*Branduardi-Raymont et al.*, 2004, 2005; *Bhardwaj et al.*, 2005a], and the Chandra X-Ray Observatory (CXO) [*Gladstone et al.*, 2002; *Elsner et al.*, 2005; A. Bhardwaj et al., manuscript in preparation, 2006]. The ROSAT observations indicated that the Jovian X rays were predominantly soft (i.e., photon energies less than 1 keV or so) with both low-latitude and high-latitude (i.e., auroral) spatial components although these components were not spatially resolved [*Waite et al.*, 1994, 1997; *Gladstone et al.*, 1998]. The total X-ray power has been observed to be roughly 1–2 GW [*Gladstone et al.*, 2002; cf. *Bhardwaj et al.*, 2002]. The auroral emission has been attributed to energetic heavy ion precipitation [*Metzger et al.*, 1983; *Waite et al.*, 1994; *Horanyi et al.*, 1988; *Cravens et al.*, 1995; *Kharchenko et al.*, 1998; *Liu and Schultz*, 1999; *Gladstone et al.*, 2002; *Cravens et al.*, 2003; *Branduardi-Raymont et al.*, 2004, 2005; *Elsner et al.*, 2005].

[3] The origin of the low-latitude X rays was not obvious, although *Waite et al.* [1997], in their interpretation of low-latitude X-ray ROSAT observations of Jupiter, suggested that low-latitude particle precipitation might be responsible for this emission. *Gladstone et al.* [1998] demonstrated that the disk-integrated intensity appeared to correlate with the F10.7 proxy for solar extreme ultraviolet (EUV) radiation. *Maurellis et al.* [2000] proposed that the low-latitude Jovian X-ray emission could be explained by the scattering of solar X-ray photons by atmospheric neutrals and by fluorescent scattering of solar X rays due to photoabsorption from the carbon K-shell. The carbon is contained in the atmospheric methane located below the homopause. The elastic contribution was shown to be more important than the K-shell contribution for Jupiter [*Maurellis et al.*, 2000], as the current paper will confirm. However, the opposite is true for Venus and Mars, where K-shell fluorescence from oxygen and carbon (species found in the dioxide atmospheres of these planets) dominates the X-ray emission

[1]Department of Physics and Astronomy, University of Kansas, Lawrence, Kansas, USA.
[2]NASA Marshall Space Flight Center, Huntsville, Alabama, USA.
[3]On leave from Space Physics Laboratory, Vikram Sarabhai Space Centre, Trivandrum, India.
[4]Department of Atmospheric, Oceanic, and Space Sciences, University of Michigan, Ann Arbor, Michigan, USA.
[5]Division of Earth-Oriented Sciences, Space Research Organization Netherlands, Utrecht, Netherlands.
[6]Southwest Research Institute, San Antonio, Texas, USA.
[7]Mullard Space Science Laboratory, University College London, Dorking, Surrey, UK.

0148-0227/06/2005JA011413

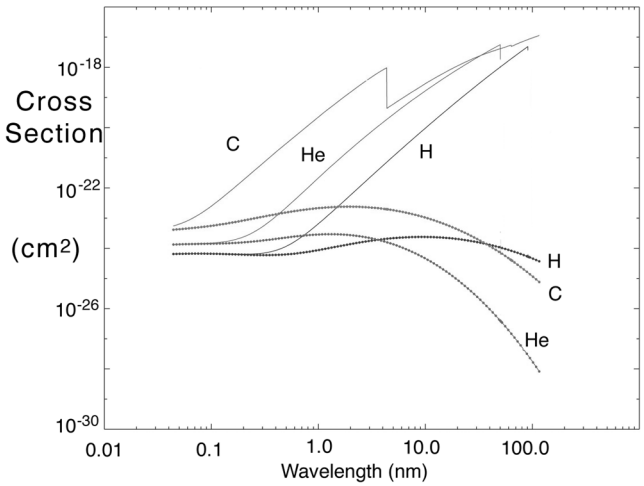

Figure 1. Elastic scattering (dotted lines) and absorption cross sections as a function of wavelength for H, He, and C. From the NIST tabulations [*Chantler*, 1995].

[*Cravens and Maurellis*, 2001; *Dennerl*, 2002; *Dennerl et al.*, 2002, 2005]. The suggestion was made that Venus can act as a diffuse mirror for solar X rays [*Dennerl et al.*, 2002], and we will demonstrate in the current paper that this is also true for Jupiter and Saturn.

[4] The CXO, with its much better spatial resolution than ROSAT, clearly revealed that the X-ray emission has two distinct components [*Gladstone et al.*, 2002]: (1) emission spread approximately uniformly over the disk (including low and middle latitudes), and (2) spatially very localized auroral emission in the polar cap at latitudes higher than the main UV auroral oval. Both components are observed to have emitted powers of roughly 1 GW. For example, *Gladstone et al.* [2002] quote values of 2.3, 1.0, and 0.4 GW for the disk X-ray power, and the north and south auroral powers, respectively, for Chandra observations made in December 2000. More recent (and longer) CXO observations have confirmed the existence of these two types of X-ray emission [*Elsner et al.*, 2005], as have recent XMM-Newton observations of Jupiter [*Branduardi-Raymont et al.*, 2004, 2005]. Both CXO [*Bhardwaj et al.*, 2004; *Elsner et al.*, 2005] and XMM-Newton [*Branduardi-Raymont et al.*, 2004, 2005] also measured spectra of the auroral and disk X rays. The auroral and disk spectra are quite different. Recently, *Bhardwaj et al.* [2005a] demonstrated that the soft X-ray emission observed from Jupiter's disk with XMM-Newton was correlated with solar X rays.

[5] Saturn is also a source of soft X rays. Emission has been observed from both low and high latitudes. Saturn's X-ray luminosity (about 300 MW) is much less than Jupiter's [*Ness et al.*, 2004a, 2004b]. *Ness and Schmitt* [2000] set upper limits for the X-ray emission from Uranus and Neptune. *Bhardwaj et al.* [2005b] recently presented CXO observations of an X-ray "flare" from Saturn that nicely correlates with a solar flare that should have been visible at Saturn as well as at Earth. *Bhardwaj et al.* [2005b] suggested that Saturn acted as a "mirror" for solar X rays and that this mirror effect could be used to detect flares from regions of the Sun not visible from the Earth. The purpose of the current paper is to follow up on the *Maurellis et al.* [2000] and *Bhardwaj et al.* [2005a, 2005b] work by presenting model calculations for elastic scattering and K-shell fluorescence scattering of solar X rays from both Jupiter and Saturn for a variety of conditions and assumed atmospheric compositions. In particular, we will explicitly calculate scattering albedos using the methods described by *Cravens and Maurellis* [2001] and *Maurellis et al.* [2000]. We suggest that measured X-ray intensities from the disk regions of Jupiter and Saturn might be useful for constraining both the absolute intensity and the spectrum of solar X rays. The solar soft X-ray irradiance spectrum is a key input for aeronomical studies of the terrestrial and planetary upper atmospheres and ionospheres [e.g., *Schunk and Nagy*, 2000].

2. Albedo for Scattering and Fluorescence of Solar X-Rays

[6] X rays can be both absorbed and elastically scattered (both incoherently and coherently) [*Chantler*, 1995] by atoms or molecules in an atmosphere. The cross sections for these processes depend on wavelength (or photon energy). Figure 1 shows atomic cross sections for absorption and scattering for H, He, and C. The cross sections for H_2 and CH_4 were assumed to be the sum of the atomic cross sections of the individual elements in the soft X ray part of the spectrum. The cross sections were taken from the NIST tabulations [*Chantler*, 1995]. Note that the scattering cross sections are much less than the absorption cross sections for the wavelengths under consideration in this paper.

[7] *Maurellis et al.* [2000] calculated the intensity of solar X rays scattered from Jupiter using these cross sections and using a model neutral atmosphere of Jupiter that included altitude profiles of molecular hydrogen, helium, and methane. The X-ray production rate was determined at each wavelength and as a function of altitude. Optical depth effects for incoming and outgoing ray paths were included. The absorption of X rays beyond the K-shell edge by carbon (in the methane) also results in X-ray emission due to K-shell fluorescence. This K-shell edge is apparent in Figure 1 at a wavelength near 4 nm [*Maurellis et al.*, 2000].

[8] *Cravens and Maurellis* [2001] used a computationally simpler approach of finding X-ray scattering and fluorescence albedos and applied this method to calculating X-ray emission from Venus and Mars. The albedo method is appropriate if two conditions are met: (1) the different atmospheric species (e.g., H_2, He, CH_4) are altitude-independent, and (2) a single scattering approximation is valid. The first condition is satisfied if the unit optical depth level for the wavelength of interest is below the homopause (below which chemically long-lived atmospheric species are uniformly mixed). Figure 2 of *Maurellis et al.* [2000] indicates that for Jupiter the unit optical depth level is located below about 350 km for wavelengths $\lambda < 12$ nm, except for solar zenith angles close to 90° (i.e., near the limb). The homopause altitude on Jupiter is located at about 350 km [cf. *Gladstone et al.*, 1998], and hence the first condition is satisfied. Satisfying the second condition requires that the scattering cross section be less than the absorption cross section. An examination of Figure 1

indicates that this condition is met for wavelengths exceeding about 0.1 nm. These conditions are also met for Saturn for wavelengths between about 0.1 nm and 100 nm.

[9] In the current paper we apply the albedo method to Jupiter and Saturn. The scattered X-ray intensity, $I_\lambda(\theta)$, at a given wavelength, λ, and at a scattering angle, θ, is the product of the solar flux at that wavelength at the top of the atmosphere (πF_λ, described later in section 3) and the wavelength and angle dependent scattering albedo $A_\lambda(\theta)$:

$$4\pi I_\lambda = A_\lambda(\theta)\pi F_\lambda \quad (1)$$

The elastic scattering albedo derived by *Cravens and Maurellis* [2001] is

$$A_\lambda(\theta) = \omega_\lambda^{tot}(\theta)\frac{1}{1+f_{io}}, \quad (2)$$

where the effective single scattering albedo is given by

$$\omega_\lambda^{tot}(\theta) = \frac{\sum_s b_s 4\pi\left(d\sigma_{s,scatt}(\lambda,\theta)/d\Omega\right)}{\sum_s b_s \sigma_{s,abs}(\lambda)}, \quad (3)$$

where $b_s = n_s/n_{tot}$ is the relative abundance of atomic species s (by volume), the number density of species s is n_s, and the total number density is n_{tot}. The absorption cross section for species s is denoted $\sigma_{s,abs}(\lambda)$ and the differential scattering cross section for species s can be written as

$$\sigma_{s,scatt}(\lambda,\theta) = \sigma_{s,scatt}(\lambda)(3/8\pi)\frac{1+\cos^2\theta}{2}, \quad (4)$$

where $\sigma_{s,scatt}$ is the total scattering cross section. The scattering angle depends on the observing geometry as does the ratio of effective pathlengths, f_{io}. Here f_{io} is equal to the ratio of the Chapman functions for the incoming (i.e., the direction to the Sun) and outgoing (i.e., the direction to the Earth) zenith angles. For the outer planets the scattering angle is within a few degrees of 180°; we adopt $\theta = 180°$. Similarly, except right near the terminator, we can adopt $f_{io} = 1$ almost everywhere on the disks of the outer planets.

[10] In the K-shell fluorescence process, photoionization of multielectron atoms by sufficiently energetic photons can remove a tightly bound electron from the K-shell, leaving a vacancy. An X-ray photon can be emitted as a high-lying valence electron makes a transition to the K-shell to fill this vacancy, although usually an Auger electron is emitted to conserve energy rather than a photon. For Jupiter and Saturn, the relevant species for this process is the carbon found in methane. The K-shell X ray yield for carbon is 0.0025 [*Krause*, 1979]. Carbon K-shell photons are produced at energies close to 0.284 keV (or wavelengths near 4.3 nm).

[11] The *Cravens and Maurellis* [2001] expression for the intensity of radiation at the K-shell wavelength, λ_K, emitted from an atmosphere due to the K-shell fluorescence process is

$$4\pi I_K = \sum_{\lambda_j<\lambda_K} A_{j,K}\ \pi F_\lambda \quad (5)$$

where $A_{j,K}$ is the albedo at wavelength λ_j (j is a bin index for a discretized solar flux) and πF_λ is the solar flux at this wavelength. *Cravens and Maurellis* [2001] derived an expression for this effective albedo. We will not reproduce this expression here, but it accounts for the fraction of photons with energies greater than the K-shell ionization threshold (wavelength λ_K) which are absorbed by carbon (rather than He or H) and then later results in the emission of K-shell X-ray photons. The expression also accounts for the possible absorption of the X-ray photon on the way out of the atmosphere. In the current paper we apply equation (5) to the outer planets.

[12] Figures 2a, 3, and 4 show the calculated albedo for elastic scattering from equation (1) as a function of wavelength and for a range of abundances. Figure 2a shows the albedos calculated for Jupiter and Saturn abundances ($He/H_2 = 17\%$ and $CH_4/H_2 = 0.25\%$ by volume for Jupiter and $He/H_2 = 6\%$ and $CH_4/H_2 = 0.2\%$ for Saturn). Note that the albedo increases with decreasing wavelength (or increasing energy) as expected from the behavior of the cross sections (Figure 1). The albedo is somewhat greater for Saturn than for Jupiter, mainly because the Jovian He abundance is higher and the He absorption cross section exceeds the hydrogen absorption cross section. The scattering cross sections for H and He are similar. The carbon K-shell edge can be seen in the albedo curves near a wavelength of 4 nm.

[13] Figure 2b shows the effective albedo for C K-shell fluorescence for Jupiter as calculated with the Cravens and Maurellis equation. As indicated by equation (5), this albedo multiplied by the solar flux for each wavelength bin and then summed (i.e., integrated) over all relevant wavelength (i.e., energy) bins gives the total intensity of X rays emitted in the carbon Kα line.

[14] Figures 3 and 4 display the elastic scattering albedo versus relative helium abundance and methane abundance, respectively, for three wavelengths. The albedo decreases with increasing helium abundance. Similarly, for wavelengths below the carbon K-shell edge, increasing methane abundance yields a lower albedo. This dependence on abundance suggests that the albedo (and scattered intensity) should be higher for observations right near the limb where the altitude of unit optical depth moves above the homopause height. The abundances of helium and methane relative to hydrogen rapidly decrease with altitude above the homopause.

3. Solar EUV and Soft X-Ray Fluxes

[15] The intensity of X rays scattered from a planet depends not only on the albedo but also on the incident solar radiation. The photon flux at a given wavelength (i.e., the solar irradiance spectrum) is denoted πF_λ (see equation (1)). *Maurellis et al.* [2000] used low solar activity irradiances (for 15 July 1994) represented with 320 wavelength bins in the EUV and soft X-ray regions of the spectrum. For λ between 3 and 12 nm, the solar irradiances from the EUV97 solar proxy model [*Tobiska and Eparvier*, 1998] were used, but for the 0.2–3 nm region of the spectrum, *Maurellis et al.* [2000] used irradiances from modeled synthetic spectra [*Mewe et al.*, 1985; *Mewe and van den Oord*, 1986] that were themselves normalized

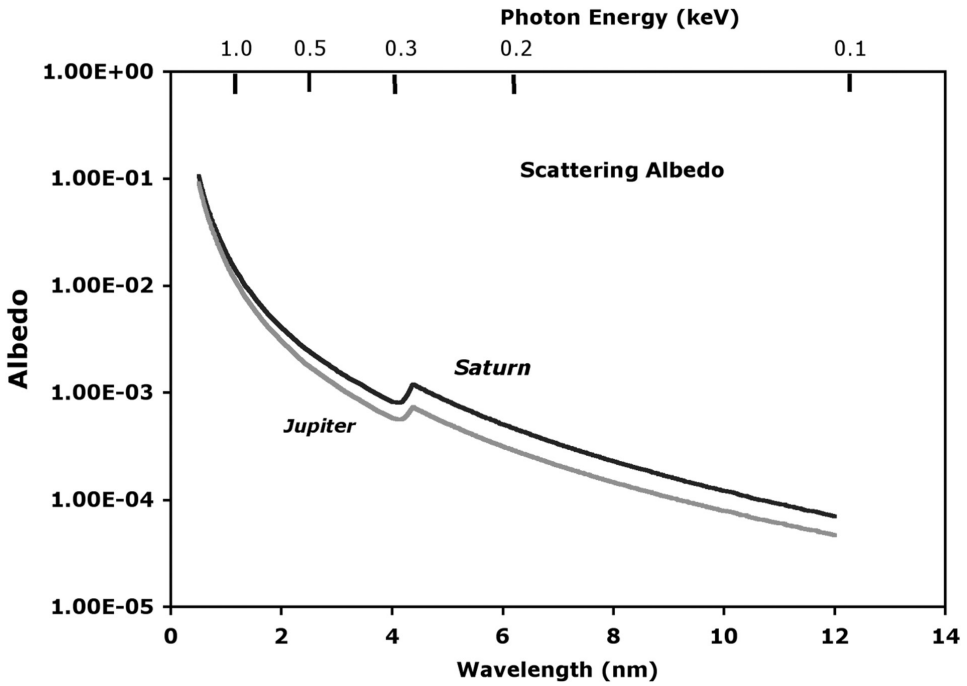

Figure 2a. Elastic scattering albedo for Jupiter and Saturn versus wavelength. The scattering angle is assumed to be 180° (appropriate for the Earth and the planet being in opposition). Photon energy is also shown on the top scale.

with Yohkoh-derived coronal color temperatures [*Acton et al.*, 1999]. This solar flux will be referred to later in the paper as the "low activity flux A" and is shown in Figure 1 of *Maurellis et al.* [2000]. F10.7 = 85.7 for this case. We also use in this paper another low solar activity irradiance spectrum (for 12 July 1994), denoted "low activity flux B." For this case, the soft X-ray flux was derived with the same methods but the irradiances for $\lambda > 3$ nm were taken from

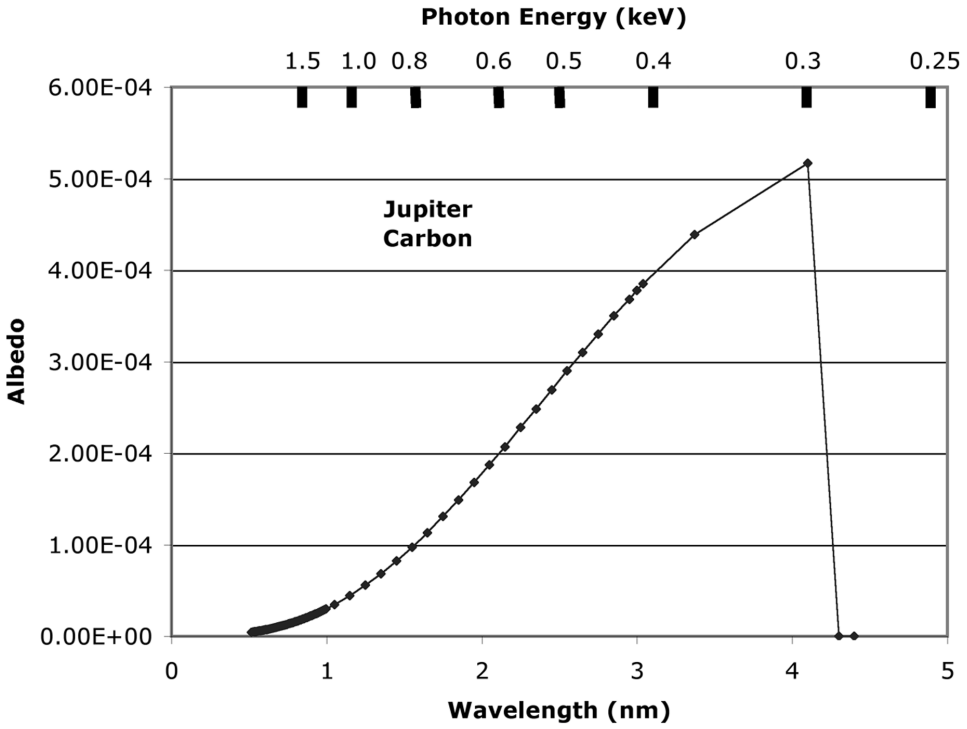

Figure 2b. Albedo as a function of wavelength for carbon K-shell fluorescence from Jupiter. Photon energy is also shown on the top scale.

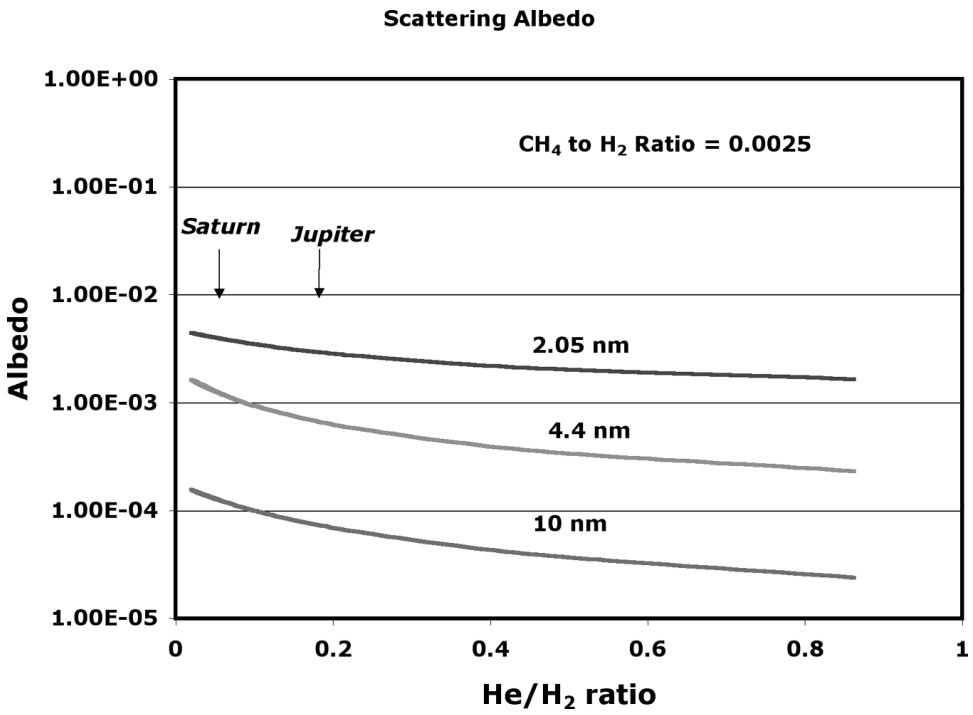

Figure 3. Elastic scattering albedo versus the fractional He to H_2 abundance for Saturnian methane abundance (CH_4/H_2 = 0.0025) (the results for the Jovian methane abundance are almost the same). The albedo is shown for three wavelengths as noted.

the more recent Solar2000 model [*Tobiska et al.*, 2000]. Figure 5 shows the irradiance spectrum. F10.7 = 83 for this case. The low activity B flux significantly exceeds the low activity A flux in the 3–5 nm part of the spectrum. A solar irradiance spectrum for "generic" high solar activity conditions (labeled "solar max" in some figures) was also constructed in the same manner, although there was some difference in the activity level we used for the soft X-ray

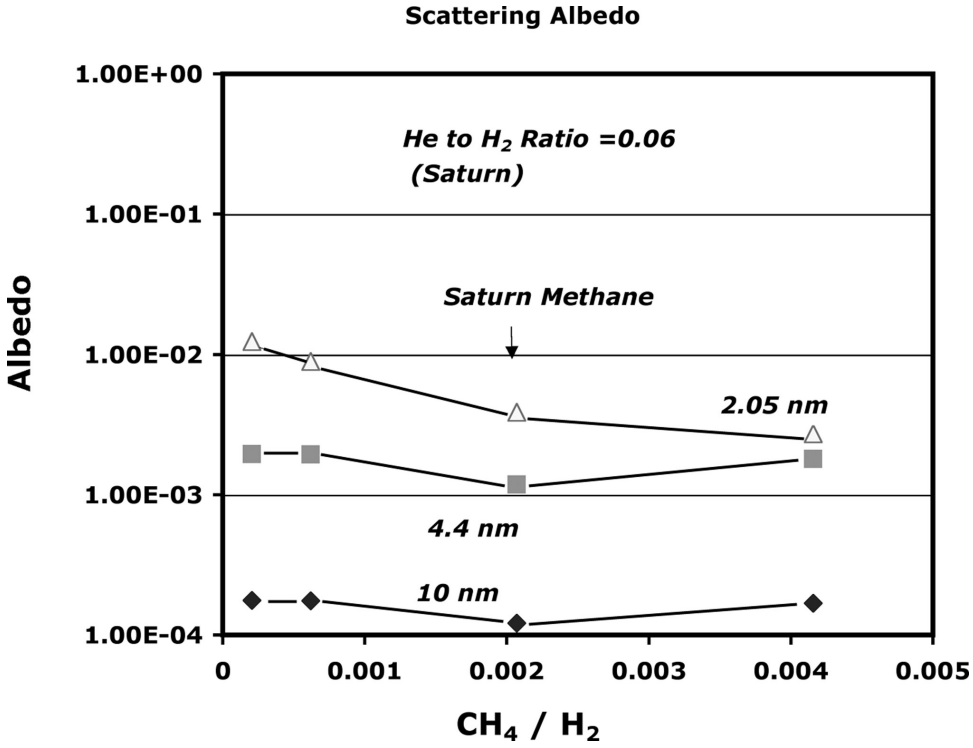

Figure 4. Elastic scattering albedo versus the methane abundance for a Saturnian helium abundance (He/H_2 = 0.06).

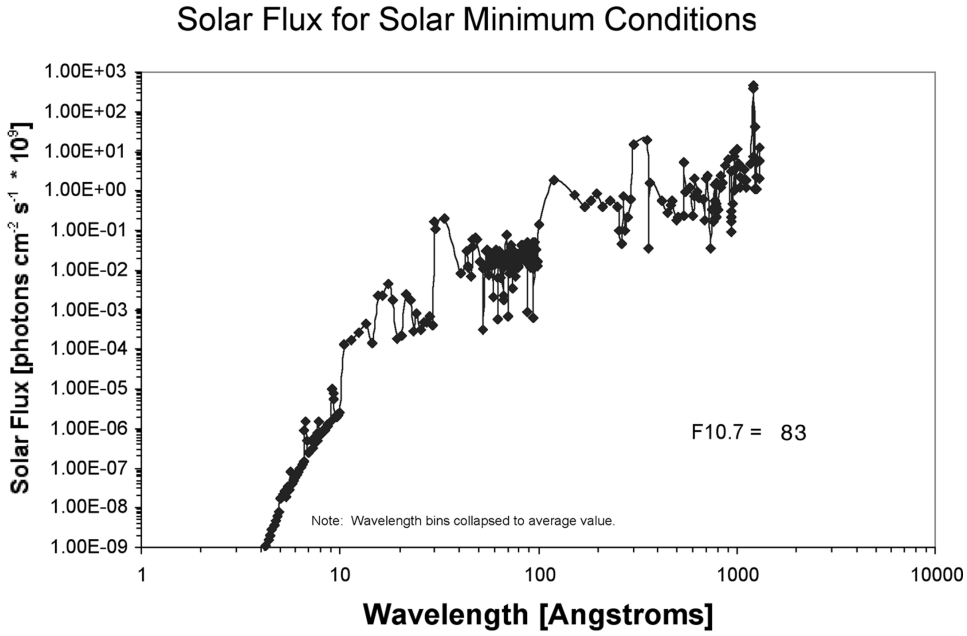

Figure 5. Solar irradiance spectra at 1 AU for low solar activity (denoted "low activity flux B" spectrum in the text.) Note: 1 angstrom = 0.1 nm.

and EUV portions of the spectrum. F10.7 = 233 for the EUV flux and F10.7 = 157 for the soft X-ray flux.

4. X-Ray Emission From the Outer Planets

[16] Equation (1) can now be used to determine scattered X-ray intensities for Jupiter and Saturn. Scattered intensities for the low activity solar spectrum A were shown by *Maurellis et al.* [2000] for Jupiter. Similar results for the solar spectrum B are shown in Figure 6. The scattered X-ray flux was also summed (i.e., averaged) over 50 eV photon energy bins for both the A and B low activity and for the high activity solar flux cases (see Figure 7). These spectra do not include the carbon K-shell line intensities from the fluorescence mechanism. Note that the intensities shown in these figures are for a situation in which Jupiter is located at a heliocentric distance of 1 AU. Obviously, the actual Jovian X-ray intensities would be less by a factor of the heliocentric distance squared (i.e., $5^2 \approx 25$). The scattered intensities calculated for Saturn for the same solar conditions (see Figure 6) look very much the same as the Jovian intensities although the actual (i.e., not scaled to 1 AU) absolute intensities are smaller by about a factor of 3. A factor of 4 is expected since Saturn is roughly twice as far from the Sun as Jupiter, but the scattering albedo for Saturn is about 50% greater than the Jovian albedo, which partially compensates for the greater distance.

[17] Table 1 lists total (i.e., summed over wavelength) scattered X-ray intensities for both Jupiter and Saturn (scaled to 1 AU distances) for several cases. Carbon K-shell line intensities are also listed in this table. For the low activity A solar flux case, the K-shell contribution relative to the total scattering intensity is only about 5%, whereas for the low activity B and high activity solar fluxes, the K-shell contribution is about 15%. This is because the latter two solar flux spectra have rather high fluxes near 3–4 nm, just below the carbon K-shell edge. However, if one just considers the total emitted X-ray power, the elastically scattered intensity dominates over the K-shell contribution for all cases. Note that the solar flux A calculations using the albedo method agree with the *Maurellis et al.* [2000] results.

[18] Table 2 lists total X-ray power densities as would be seen at Earth, both from our model and from various

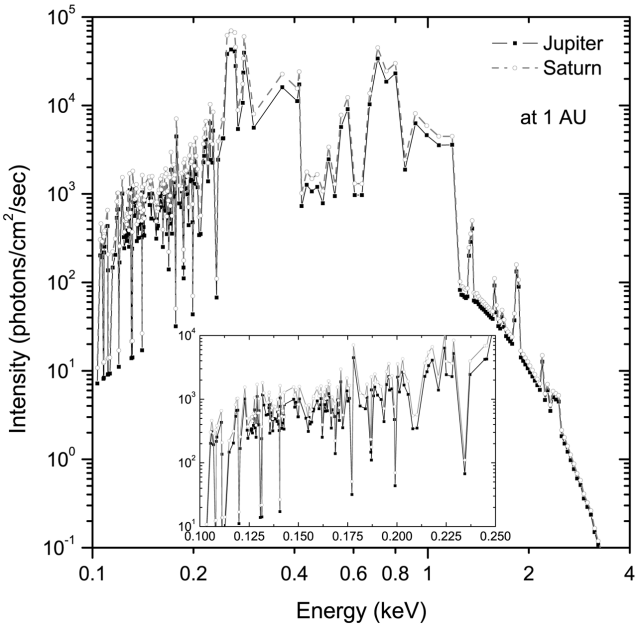

Figure 6. Scattered Jovian and Saturnian X-ray intensities (normalized for 1 AU) versus photon energy at high resolution. The spectrum does not include the carbon K-shell line intensities from the fluorescence mechanism. The intensity points are "per bin." The inset is an expanded view of the low energy spectra.

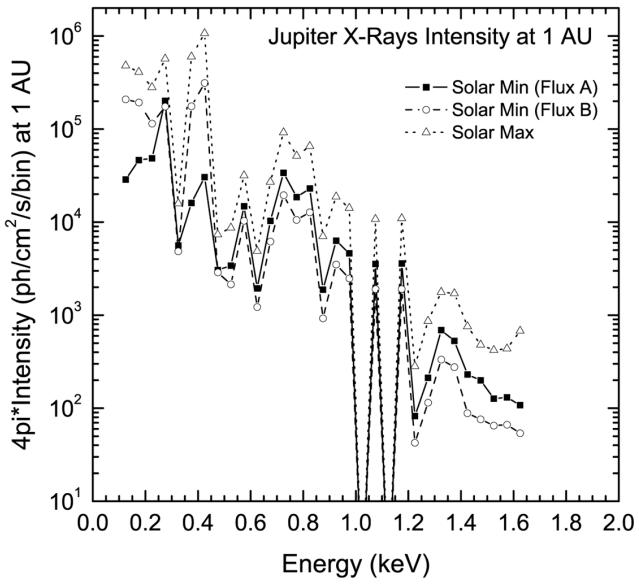

Figure 7. Scattered Jovian X-ray intensity (normalized for 1 AU) versus photon energy at 50 eV-resolution for two different low solar activity solar fluxes, as well as the high solar activity case (''solar max''). Each bin is 50 eV wide for this figure. The spectra do not include the carbon K-shell line intensities from the fluorescence mechanism. The two ''gaps'' near 1 keV and 1.1 keV are due to the lack of solar intensity points for these energy intervals rather than due to any intrinsic structure in the spectrum.

observations available in the literature. For simplicity, we have adopted typical Jovian and Saturnian heliospheric distances of 5.2 AU and 9.5 AU, respectively, when scaling the model results to compare with the observations. We have also used these values for the Earth-planet distances. In fact, however, these distances can differ from these values by as much as 20% depending on the specific observational geometry, and this effect could have as much as 40% effect on the calculated powers. A careful comparison of a model calculation with a specific observation requires that distances consistent with the time of this observation be used. However, the current accuracy of the model and our limited knowledge of the input solar spectrum introduce even greater uncertainties at this time. For equivalent solar activity levels (i.e., for the same input solar flux levels), we find that the X-ray flux observed at Earth from Saturn is ≈10 times less than for Jupiter. A factor of ≈12 would be expected for identical albedos, but Saturn has a somewhat higher scattering albedo than Jupiter.

[19] Some measured X-ray powers for Jupiter and Saturn are also provided in Table 2. For a given observation, the power value was placed in the column of the table according to the appropriate solar activity level (i.e., F10.7) with lower values being to the left. A more complete compilation of observed ''disk'' (i.e., nonauroral) X-ray powers for Saturn was provided by *Bhardwaj et al.* [2005b], who demonstrated a good correlation between X ray production and solar activity. Such a solar activity dependence of the disk X-ray power is also evident in Table 2 for both planets. An examination of Table 2 indicates that the observed X-ray intensities agree reasonably well (i.e., at roughly the 50% level) with the appropriate model intensities, particularly in the solar activity trends and in the Jupiter-Saturn differences, although as mentioned earlier the model results only used ''typical'' heliocentric and planetary distances rather than values tuned to each observation.

Table 1. Spectrally Summed Soft X-Ray Intensities for Jupiter and Saturn at 1 AU Calculated With the Model[a]

Source (Wavelength)	Low Activity A	Low Activity B	High Activity
	Jupiter		
Elastic (0.2–12 nm)	0.51	1.26	3.79
Carbon K-shell (4.4 nm)	0.028	0.20	0.68
Total	0.54	1.46	4.47
	Saturn		
Elastic (0.2–12 nm)	0.77	1.89	5.62
Carbon K-Shell (4.4 nm)	0.037	0.26	0.90
Total	0.81	2.15	6.52

[a]Here 4π I (in units of Rayleighs) are shown, where I is the intensity (units of cm^{-2} s^{-1} sr^{-1}). Note: *Maurellis et al.* low activity A case: total intensity = 0.56 R. Note: 1 Rayleigh (R) = 10^6 cm^{-2} $s^{-1}$and the units of intensity are cm^{-2} s^{-1} sr^{-1}.

5. X-Ray Spectra of the Disks of the Outer Planets

[20] The scattered solar spectrum, like the incident solar spectrum, is expected to contain discrete line emission from

Table 2. Total Soft X-Ray Fluxes From Jupiter and Saturn As Observed at Earth: Model Results and Observations[a]

Source (Energy)	Low Activity A F10.7 = 86	Low Activity B F10.7 = 83	High Activity F10.7 = 157–233
	Jupiter		
Elastic 0.1–1.7 keV			
(No K-shell)	2.49	4.88	16.2
(With K-shell)	2.59	5.59	18.6
Elastic, 0.3–1.7 keV	1.52	3.22	11.8
ROSAT,[b] 0.1–0.55 keV; disk = 50% total			15
XMM,[c] 0.3–2 keV		4	
CXO, 0.5–1.5 keV (this paper)		5.38	
	Saturn		
Elastic, 0.1–1.7 keV			
(No K-shell)	0.25	0.50	1.66
(With K-shell)	0.26	0.57	1.89
Elastic, 0.3–1.7 keV	0.14	0.31	0.66
ROSAT,[b] 0.1–0.55 keV; disk and aurora			1.9
XMM,[d] 0.1–2 keV			1.6
CXO,[e] 0.1–2 keV		0.68	
CXO,[f] 0.23–2 keV, 0.34–2 keV		0.43	1.27

[a]Power density, 10^{-14} erg cm^{-2} s^{-1}.
[b]*Ness and Schmitt* [2000].
[c]*Branduardi-Raymont et al.* [2004].
[d]*Ness et al.* [2004a].
[e]*Ness et al.* [2004b].
[f]*Bhardwaj et al.* [2005b].

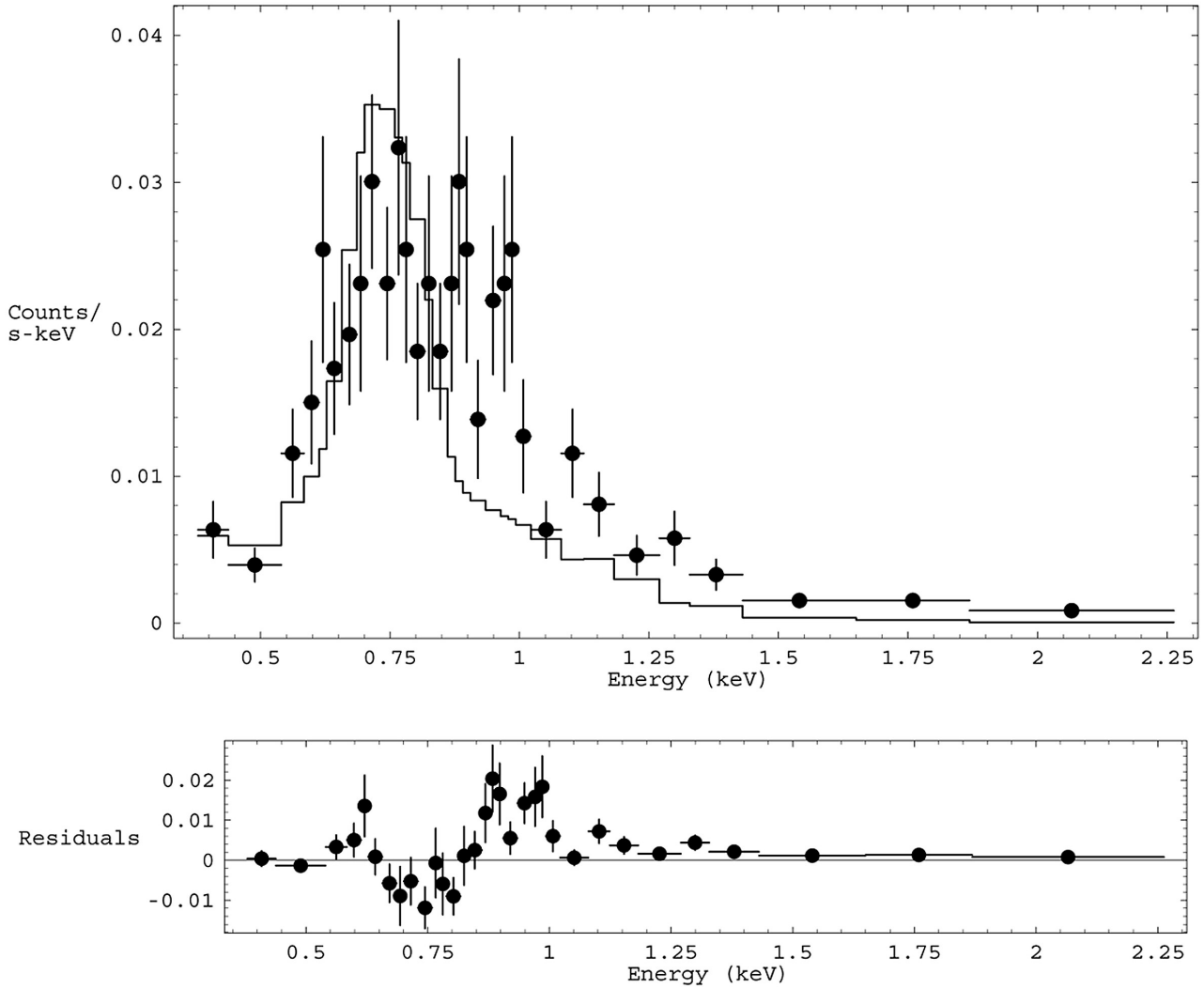

Figure 8. Comparison of measured and modeled disk X-ray spectra for Jupiter. The modeled count rates are for the solar "low activity flux A" case and are generated by convolving our model with the CXO ACIS-S instrumental response. The model includes the carbon K-shell line intensities. The data shown are from CXO ACIS-S measurements of Jupiter's disk (i.e., auroral regions are excluded) during February 2003 (see the paper in preparation by Bhardwaj et al. for details of the observations; the auroral data from this same set of CXO observations are described by *Elsner et al.* [2005]).

a very large number of atomic transitions. And given that the solar flux is highly time-variable, especially in the X ray part of the spectrum, then the Jovian and Saturnian disk spectra should also be highly time-variable. Disk spectra have been measured for Saturn [*Ness et al.*, 2004a, 2004b; *Bhardwaj et al.*, 2005b]. Particularly high count rates are evident in the 0.6 to 1 keV part of the planetary disk spectra, which is consistent with the model spectra shown earlier. For Jupiter, the disk spectra measured by XMM-Newton and CXO differ substantially from the spectra observed in the auroral regions [*Branduardi-Raymont et al.*, 2004, 2005; *Bhardwaj et al.*, 2004; *Elsner et al.*, 2005]. The auroral intensities are (relatively) much higher near energies of 0.6 keV and 0.3–0.4 keV than are the disk spectra [*Branduardi-Raymont et al.*, 2004, 2005; *Elsner et al.*, 2005]. The Jovian and Saturnian disk spectra are quite similar.

[21] In this paper, we show comparisons of model disk spectra with spectra measured for Jupiter by the Chandra ACIS-S instrument. Figure 8 shows these comparisons for the solar flux A ("old solar min.") model cases. The solar spectrum B only makes a significant difference for the comparison at energies below 0.4 keV (see Figure 7), and a data comparison is not shown. The Chandra spectrum for Jupiter was taken on 24 February 2003, and the auroral regions were excluded from the data being shown here. The daily F10.7 index for the solar flux was 102 for this date (corrected for light travel time). A more detailed discussion of these measurements will be presented in another (companion) paper now in preparation (A. Bhardwaj et al., manuscript in preparation, 2006). The model intensities used in these figures were the 50 eV average values (see Figure 7), convolved with the ACIS-S energy-dependent instrumental response function. The carbon K-shell line intensities were included. The fit gave a reduced chi-squared value of 3.20.

[22] The measured and modeled soft X-ray spectra are similar in their general shape, although the model intensities

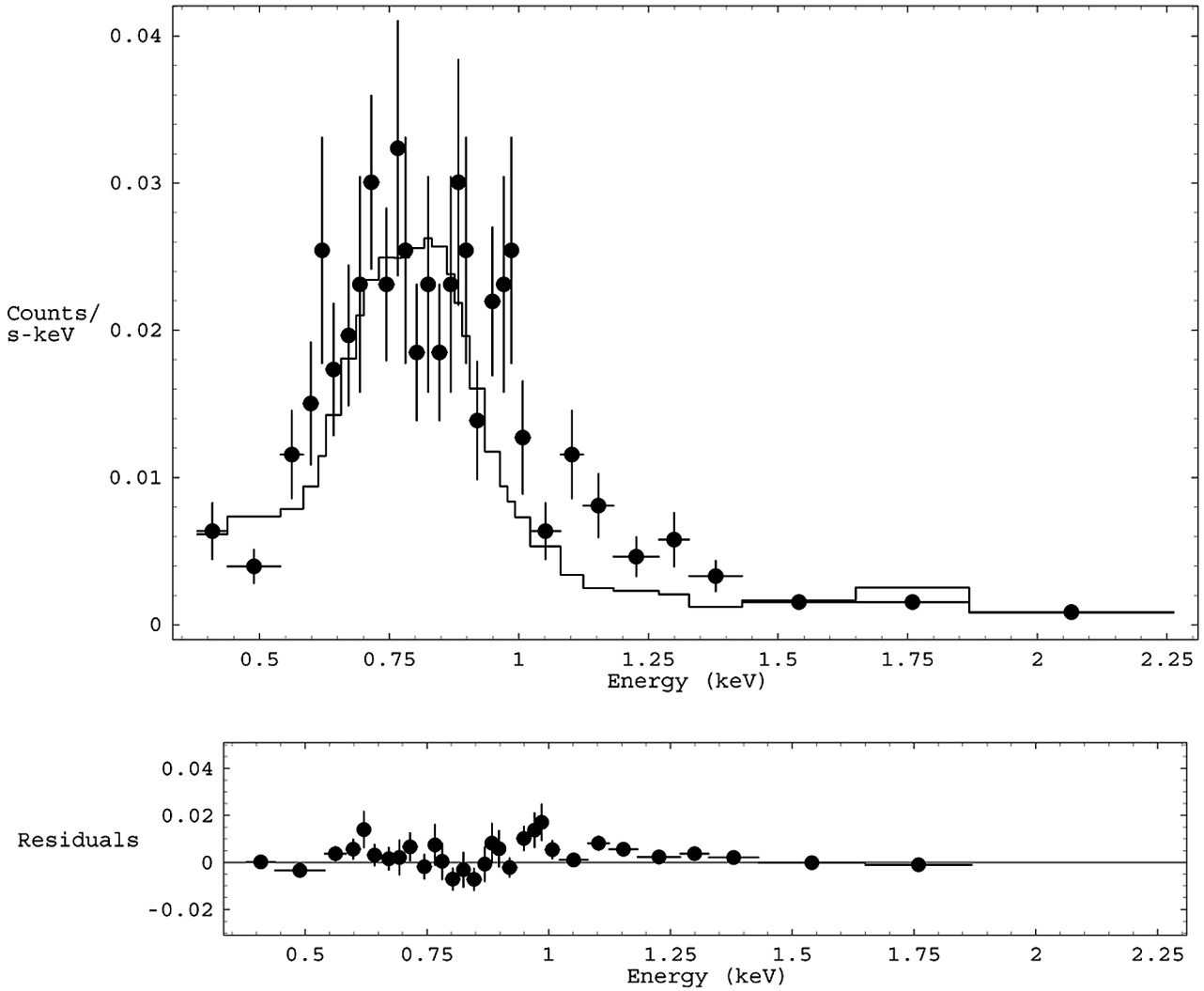

Figure 9. The CXO data is the same as in Figure 8, CXO ACIS spectrum of the Jovian disk (auroral regions excluded), but for this figure the comparison is with a MEKAL collisional plasma model intensity multiplied by the Jovian X-ray scattering albedo and convolved with the instrumental response function.

are about a factor of 2 lower than the measured values in the 0.8–1.2 keV energy range. Both the predicted and measured fluxes in the spectra increase toward low energies below 0.4 keV and both have a broad peak between 0.6 and 0.8 keV. A line appears in the measured spectrum at an energy of 1.35 keV. This line also appears in the model spectra shown in Figures 6 and 7 and is due to a strong line in the solar spectrum (the coronal MgXI line), but the line is "washed out" after the model spectrum is convolved with the rather broad ACIS response function.

[23] Figure 9 shows a comparison of a CXO ACIS spectrum from the February 2003 observations of Jupiter with intensities calculated with a MEKAL model (see the XSPEC manual online at http://xspec.gsfc.nasa.gov/docs/xanadu/xspec/manual/manual.html) multiplied by the Jovian scattering albedo. The abundances used in the MEKAL model were held fixed at solar values, but the temperature was allowed to vary and a temperature of kT = 0.593 keV gave the best fit over the energy range 0.4–2.0 keV with a reduced chi-squared value of 2.32. The total energy flux in the 0.5–1.5 keV range for this model fit was 5.38×10^{-14} erg cm^{-2} s^{-1} (as observed at Earth; note, though, that the model intensities are lower than the measured values in the 0.8–1.2 keV energy range). Just as with the earlier model comparison, the agreement in Figure 9 between the model and the data is good in the 0.4–0.8 keV part of the spectrum but at higher energies the model intensities are too low.

6. Discussion and Conclusions

[24] *Maurellis et al.* [2000] proposed that low-latitude soft X-ray emission from Jupiter could be explained by the scattering of solar X rays. In this paper we determined the soft X-ray emission from the disks of Jupiter and Saturn using both existing EUV solar flux data [*Tobiska and Eparvier*, 1998] and collisional equilibrium models of the solar corona combined with Yohkoh observations of the Sun [*Acton et al.*, 1999]. The scattered radiation in our models depends on the solar X-ray flux and on the scattering

albedo. That is, Jupiter and Saturn act as diffuse mirrors (albeit low reflectivity ones), as suggested by *Bhardwaj et al.* [2005a, 2005b].

[25] Several characteristics of the observed X-ray emission from the disks of Jupiter and Saturn support this suggestion, although it cannot be claimed yet that this process is fully understood. First, the nonauroral X-ray intensities observed from Jupiter or Saturn appear to be at least approximately uniformly-distributed spatially [*Gladstone et al.*, 2002; *Elsner et al.*, 2005; *Branduardi-Raymont et al.*, 2004; *Ness et al.*, 2004a, 2004b; *Bhardwaj et al.*, 2005a, 2005b], as would be predicted by equation (1) for an outer planet for which both the factor f_{io} and the scattering angle, θ, do not vary much across the disk. Second, the disk intensities appear to correlate with the solar X-ray flux, or at least with the F10.7 proxy index of solar activity [*Gladstone et al.*, 1998; *Maurellis et al.*, 2000; *Bhardwaj et al.*, 2005a, 2005b]. Third, as mentioned in the previous section (see Table 2), the Jupiter-Saturn disk intensity ratio is roughly what one would expect for a solar-related mechanism. Fourth, the observed disk X-ray spectra for Jupiter and Saturn are broadly consistent with scattered solar X rays (as shown in Figures 8 and 9).

[26] However, the details of the disk soft X-ray spectra are not fully understood yet, that is, why are the model intensities too low for energies above 0.8 keV? One possibility is that the solar irradiance spectra adopted (i.e., the solar A model for Figure 8 or the MEKAL model for Figure 9) do not adequately (at least for photon energies above about 0.8 keV) represent the actual solar spectrum for the time and circumstances of the CXO observations. Another possibility is that scattering of solar radiation does not fully account for all of the disk emission and that an X-ray source intrinsic to Jupiter also exists. In the latter case, there should be hints in the spatial morphology of the emission, which should be further studied to check for quantitative consistency with the scattering hypothesis; this will be pursued in a later paper (A. Bhardwaj et al., manuscript in preparation, 2006).

[27] *Ness and Schmitt* [2000] used ROSAT observations to set 95% confidence upper limits to the soft X-ray energy flux from Uranus and Neptune of 5.7×10^{-15} and 4.7×10^{-15} ergs cm^{-2} s^{-1}, respectively. With the assumption that all the emission from these planets is due to scattered solar X-rays (and using Jovian albedo values and the high solar activity solar flux case), we predict soft X-ray fluxes from Uranus and Neptune of 1.3×10^{-16} and 2.0×10^{-17} ergs cm^{-2} s^{-1}, respectively. These model values are much less than the *Ness and Schmitt* [2000] upper limits for these planets and so are not in conflict with them. A search for X rays from Uranus using Chandra on 7 August 2002, has also yielded negative results (Obs ID = 2518 with 30 ks exposure time; A. Metzger, private communication, 2005).

[28] Solar extreme ultraviolet and soft X-ray photons are the major source of energy for the upper atmospheres and ionospheres of solar system bodies [*Schunk and Nagy*, 2000]. Quoting from page 241 of *Schunk and Nagy* [2000]: "Solar radiation in the EUV and x-ray range of wavelengths excites, dissociates, and ionizes the neutral constituents in the upper atmosphere." Hence the solar EUV and X-ray irradiance spectrum play an important role in the field of aeronomy. A number of solar flux models have been used over the years [cf. *Schunk and Nagy*, 2000], but a continuing need exists for better and more accurate solar flux data, partly because the solar flux is so highly variable and because the spectrum is so complex [e.g., *Tobiska*, 1991; *Hinteregger et al.*, 1981; *Tobiska and Eparvier*, 1998; *Warren et al.*, 1998]. Perhaps, when the scattering process is understood somewhat better, observations of disk emission from the outer planets could serve as an important supplement to the current sources of information on the solar soft X-ray flux, particularly for regions of the solar disk not visible from the Earth.

[29] **Acknowledgments.** We thank L. W. Acton (Montana State University) for providing solar soft X-ray irradiances. NASA Planetary Atmospheres grant NNG04GQ58G and NSF Solar Terrestrial Physics grant ATM-0234271 (TEC) are gratefully acknowledged. A part of this research was conducted when A. Bhardwaj held the NRC Senior Research Associateship at NASA Marshall Space Flight Center.

[30] Arthur Richmond thanks the reviewers for their assistance in evaluating this paper.

References

Acton, L. W., D. C. Weston, and M. E. Bruner (1999), Deriving solar X ray irradiance from *Yohkoh* observations, *J. Geophys. Res.*, *104*, 14,827.

Bhardwaj, A., et al. (2002), Soft X-ray emissions from planets, moons, and comets, *Eur. Space Agency Spec. Publ., ESA-SP-514*, 215–226.

Bhardwaj, A., et al. (2004), Chandra X-ray observations of Jovian low latitude emissions: Morphological, temporal and spectral characteristics, *Bull. Am. Astron. Soc.*, *36*(4), 18.04.

Bhardwaj, A., G. Branduardi-Raymont, R. F. Elsner, G. R. Gladstone, G. Ramsay, P. Rodriguez, R. Soria, J. H. Waite Jr., and T. E. Cravens (2005a), Solar control on Jupiter's equatorial emissions: 26–29 November 2003 XMM-Newton Observation, *Geophys. Res. Lett.*, *32*, L03S08, doi:10.1029/2004GL021497.

Bhardwaj, A., R. F. Elsner, J. H. Waite Jr., G. R. Gladstone, T. E. Cravens, and P. Ford (2005b), X-ray flare and aurora at Saturn, *Astrophys. J. Lett.*, *624*, L121–L124.

Branduardi-Raymont, G., et al. (2004), First observation of Jupiter by XMM-Newton, *Astron. Astrophys.*, *424*, 331.

Branduardi-Raymont, G., A. Bhardwaj, R. Elsner, G. Gladstone, G. Ramsay, P. Rodriguez, R. Soria, J. H. Waite, and T. E. Cravens (2005), X-ray exploration of the giant planets, their magnetospheres and the solar connection: From XMM-Newton to XEUS, in *Trends in Space Science and Cosmic Vision 2020*, *Eur. Space Agency Spec. Publ.*, *ESA SP-588*, 393.

Chantler, C. T. (1995), Theoretical form factor, attenuation, and scattering tabulation for Z = 1–92 from E = 1–10 eV to E = 0.4–1.0 MeV, *J. Phys. Chem. Ref. Data*, *24*, 71.

Cravens, T. E., E. Howell, J. H. Waite, and G. R. Gladstone (1995), Auroral oxygen precipitation at Jupiter, *J. Geophys. Res.*, *100*, 14,827.

Cravens, T. E., and A. N. Maurellis (2001), X-ray emission from scattering and fluorescence of solar x-rays at Venus and Mars, *Geophys. Res. Lett.*, *28*, 3043.

Cravens, T. E., et al. (2003), Implications of Jovian X-ray emission for magnetosphere-ionosphere coupling, *J. Geophys. Res.*, *108*(A12), 1465, doi:10.1029/2003JA010050.

Dennerl, K. (2002), Discovery of x-rays from Mars with Chandra, *Astron. Astrophys.*, *394*, 1119.

Dennerl, K., V. Borwitz, J. Englhauser, C. Lisse, and S. Wolk (2002), Discovery of x-rays from Venus with Chandra, *Astron. Astrophys.*, *386*, 319.

Dennerl, K., C. M. Lisse, A. Bhardwaj, V. Burwitz, J. Englhauser, H. Gunnel, M. Holmstrom, F. Jansen, V. Kharchenko, and P. M. Rodriquez-Pascual (2005), Mars observed with XMM-Newton: High resolution X-ray spectroscopy, *Astron. Astrophys.*, in press.

Elsner, R. F., et al. (2002), Discovery of soft X-ray emission from Io, Europa, and the Io plasma torus, *Astrophys. J.*, *572*, 1077.

Elsner, R. F., et al. (2005), Simultaneous Chandra X-ray, HST ultraviolet, and Ulysses radio observations of Jupiter's aurora, *J. Geophys. Res.*, *110*, A01207, doi:10.1029/2004JA010717.

Gladstone, G. R., J. H. Waite Jr., and W. S. Lewis (1998), Secular and local time dependence of Jovian X ray emissions, *J. Geophys. Res.*, *103*, 20,083.

Gladstone, G. R., et al. (2002), A pulsating auroral X-ray hot spot on Jupiter, *Nature*, *415*, 1000.

Hinteregger, H. E., K. Fukui, and B. R. Gibson (1981), Observational, reference, and model data on solar EUV, from measurements on AE-E, *Geophys. Res. Lett.*, *8*, 1147.

Horanyi, M., T. E. Cravens, and J. H. Waite Jr. (1988), The precipitation of energetic heavy ions into the upper atmosphere of Jupiter, *J. Geophys. Res.*, *93*, 7251.

Kharchenko, V., W. Liu, and A. Dalgarno (1998), X-ray and EUV emission spectra of oxygen ions precipitating into the Jovian atmosphere, *J. Geophys. Res.*, *103*, 26,687.

Krause, M. O. (1979), Atomic radiation and radiationless yields for K and L shells, *J. Phys. Chem. Ref. Data*, *8*, 307.

Liu, W., and D. R. Schultz (1999), Jovian X-ray aurora and energetic oxygen precipitation, *Astrophys. J.*, *526*, 538.

Maurellis, A. N., T. E. Cravens, G. R. Gladstone, J. H. Waite, and L. W. Acton (2000), Jovian X-ray emission from solar X-ray scattering, *Geophys. Res. Lett.*, *27*, 1339.

Metzger, A. E., et al. (1983), The detection of X rays from Jupiter, *J. Geophys. Res.*, *88*, 7731.

Mewe, R., E. H. N. M. Gronenschild, and G. H. J. van den Oord (1985), Calculated X-radiation from optically thin plasmas, Paper V, *Astron. Astr. Suppl.*, *62*, 197.

Mewe, R., and G. E. J. van den Oord (1986), Calculated x-radiation from optically thin plasmas, paper VI, *Astron. Astr. Suppl.*, *65*, 511.

Ness, J.-U., and J. H. M. M. Schmitt (2000), A search for X-ray emission from Saturn, Uranus, and Neptune, *Astron. Astrophys.*, *335*, 394.

Ness, J.-U., J. H. M. M. Schmitt, S. J. Wolk, K. Dennerl, and V. Burwitz (2004a), X-ray emission from Saturn, *Astron. Astrophys.*, *418*, 337.

Ness, J.-U., J. H. M .M. Schmitt, and J. Robrade (2004b), Detection of Saturnian X-ray emission with XMM-Newton, *Astron. Astrophys.*, *414*, L49.

Schunk, R. W., and A. F. Nagy (2000), *Ionospheres*, Cambridge Univ. Press, New York.

Tobiska, W. K. (1991), Revised solar extreme ultraviolet flux model, *J. Atmos. Terr. Phys.*, *53*, 1005.

Tobiska, W. K., and F. G. Eparvier (1998), EUV97: Improvements to EUV irradiance modeling in the soft X rays and FUV, *Solar Physics*, *177*, 147.

Tobiska, W. K., T. Woods, F. Eparvier, R. Viereck, L. Floyd, D. Bouwer, G. Rottman, and O. R. White (2000), The SOLAR2000 empirical solar irradiance model and forecast tool, *J. Atmos. Sol. Terr. Phys.*, *62*, 233.

Waite, J. H., et al. (1994), ROSAT observations of the Jupiter aurora, *J. Geophys. Res.*, *99*, 14,799.

Waite, J. H., et al. (1997), Equatorial X-ray emissions: Implications for Jupiter's high exospheric temperatures, *Science*, *276*, 104.

Warren, H. P., J. T. Mariska, and J. Lean (1998), A new reference spectrum for the EUV irradiance of the quiet Sun: 2. Comparisons with observations and previous models, *J. Geophys. Res.*, *103*, 12,091.

A. Bhardwaj and R. Elsner, NASA Marshall Space Flight Center, NSSTC/XD12, 320 Sparkman Drive, Huntsville, AL 35805, USA. (anil.bhardwaj@msfc.nasa.gov; ron.elsner@msfc.nasa.gov)

G. Branduardi-Raymont, Mullard Space Science Laboratory, University College London, Holmsbury St. Mary, Dorking, Surrey, UK.

J. Clark and T. E. Cravens, Department of Physics and Astronomy, University of Kansas, Lawrence, KS 66045, USA. (cravens@ku.edu)

G. R. Gladstone, Southwest Research Institute, P. O. Drawer 28510, 6220 Culebra, San Antonio, TX 78284, USA. (randy.gladstone@swri.org)

A. N. Maurellis, Division of Earth-Oriented Sciences, Space Research Organization Netherlands, Sorbonnelaan 2, 3584 CA Utrecht, Netherlands. (ahilleas@gmail.com)

J. H. Waite Jr., Department of Atmospheric, Oceanic, and Space Sciences, University of Michigan, 2455 Hayward, Ann Arbor, MI 48105, USA. (hunterw@umich.edu)